PCCP

Accepted Manuscript

ROYAL SOCIETY OF CHEMISTRY

www.rsc.org/pccp

PCCP RSCPublishing

Paper

Inhibited Phase Behavior of Gas Hydrate in Graphene Oxide: Influences of Surface and Geometric Constraint

Cite this: DOI: 10.1039/x0xx00000x

Received 00th January 2012,
Accepted 00th January 2012

DOI: 10.1039/x0xx00000x

www.rsc.org/

Daeok Kim,[a‡] Dae Woo Kim,[b‡] Hyung-Kyu Lim,[a] Jiwon Jeon,[a] Hyungjun Kim,[a]
Hee-Tae Jung,[b★] and Huen Lee[ab★]

Porous materials have provided unprecedented opportunities to develop emerging technologies such as molecular storage systems and separation mechanisms. Pores also have been used as support to contain gas hydrate for the application in gas treatments. Necessarily, exact understanding on the properties of gas hydrate in confining pores is important. Here, we investigated the formation of CO_2, CH_4 and N_2 hydrate in non-interlamellar voids in graphene oxide (GO), and their thermodynamic behaviors. For that, low temperature XRD and P-T traces were conducted to analyze water structure and confirm hydrate formation, respectively, in GO after its exposure to gaseous molecules. Confinement and strong interaction of water with the hydrophilic surface of graphene oxide reduce water activity, which leads to the inhibited phase behavior of gas hydrates.

Introduction

The inclusion of gas molecules in the hydrogen-bonded water frameworks of hydrates has created the potential for a variety of interesting applications in energy storage and transportation, carbon dioxide sequestration, and molecular separation. Specifically, hydrate-based CH_4 storage and transportation might provide positive advantages in safety during gas storage processes and lead to much lower capital cost compared to current liquefied natural gas techniques.[1]

A distinct competition for occupancy in hydrate cages, between dissimilar guest molecules, has made it possible to establish hydrate-based gas separation.[2] In particular, such a separation technology using highly preferential selectivity in hydrate cages may provide for effective separation of troublesome CO_2 from various emission sources (e.g., power plants). This potential is due to the greater affinity of CO_2 to enter hydrate cages, compared to other gases.[3] As might be expected, the real process appears to be quite simple. The CO_2 in gas mixtures is selectively enriched by enclosure in the solid-hydrate phase and the captured CO_2 can later readily be recovered by dissociating the CO_2 from the hydrate.

However, despite the inherent merits of using gas hydrates in commercially viable processes, a few issues remain that should be properly resolved. These include mitigation of harsh working conditions (high pressure and low temperature), control of hydrate formation and dissociation rates, and achievement of high separation selectivity. Previous research on gas hydrates confined in porous media has demonstrated the increased separation selectivity for CO_2, faster hydrate growth than in the bulk state.[4] Also CH_4 hydrate formation in ZIF-8, a sort of microporous material, increased storage capacity of CH_4.[5] Moreover, the hydrate formation achieved in micro-porous networks does not require solution stirring. This process is essential for favorable contact of water with gas in bulk water, otherwise hydrate films formed at the interface between water and gas would seriously interfere with hydrate growth. However, the peculiar and unique gas inclusions occurring in the confined surrounding have not been closely explored in spite of the importance of such study for revealing the mechanism of crystalline hydrate growth and for further developing various hydrate-based gas storage and separation processes.

Here, we examined the guest dynamics and phase behavior of CO_2, CH_4, and N_2 hydrates formed in confined non-interlamellar voids in graphene oxide (GO). As shown in Fig. 1a, a single layer of GO is a 2-dimensional oxidized carbon sheet, where the surface is covered with ether, hydroxyl and carboxylic acid functional groups.[6] The stacking of GO layers leads to GO particles wherein pore spaces exist as either interlayer or non-interlamellar voids. The highly functionalized GO surface interacts strongly with water molecules and can include water molecules in both kinds of voids.[7] Water structuring in swollen GO particles is depicted in Fig. 1b. Previous research on water dynamics in GO has revealed that the interaction pattern of water with neighboring surfaces and

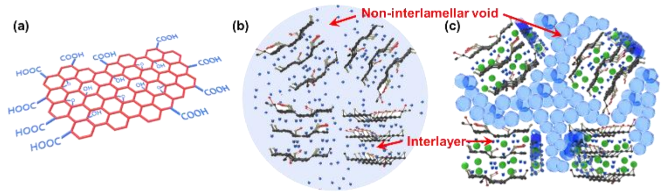

Fig. 1 Schematic description of (a) GO sheet, (b) water swollen GO particles, and (c) GO with gas hydrate in non-interlamellar voids, where blue circles indicate gas hydrate structure.

voids is strongly affected by the water concentration. Water mainly exists in interlayer spaces at water concentrations lower than 25 wt% and doesn't crystallize.[7b] In the interlayer spaces, water shows dynamics, such as reduced translational and rotational motion, that are more restricted than for bulk water due to its strong interaction with functional groups on surfaces.[7] In contrast, at water concentrations higher than ~25 wt%, water can serve the role of intercalated water, as well as of confined water in non-interlamellar voids. Within the non-interlamellar voids, water can readily crystallize and transform to solid water structures such as hexagonal ice (the most energetically stable form). At this stage, we note that non-stoichiometric GO can change slightly, according to the procedure used in its synthesis. Accordingly, the criterion of 25% water concentration cannot be applied to all the GO that should be considered for this kind of research.

Herein, to research the potential use of GO for gas storage and separation, we examined the physical and chemical characteristics of gas hydrates formed from non-interlamellar water as described in Fig. 1c. Moreover, we checked to see whether the pores in GO influences, to some degree, the hydrate formation. The structural observation of gas hydrates growing in GO were conducted using low-temperature XRD. The phase behavior of CO_2 and CH_4 hydrates confined within the unique locations within GO was explored using isochoric pressure-temperature trace curves.

Experimental section

Graphene oxide was synthesized using a modified Hummers method.[6] Graphite powder (1 g, Asbury Carbon) was added to sulfuric acid (98%, 150 mL), which served as a solvent. Potassium permanganate (99.0%, 2.5 g), employed as an oxidizing agent, was gradually added to the graphite solution, with vigorous stirring for about 10 minutes. After reaction at 308 K for 2 h, the solution was cooled in an ice bath and diluted with 200 mL of deionized water. Following 4 h of stirring, 100 mL of hydrogen peroxide was added to the reaction solution. The mixture was then filtered with a glass filter and washed several times with hydrochloric acid (10 %). After this washing process, the remaining solvent was evaporated under vacuum at room temperature for 12 h. The dried GO was crushed using a blender to achieve particle size smaller than 100 um. The pore properties of GO was analyzed through argon adsorption using an ASAP 2020 physisorption analyzer (Micromeritics, USA) at the Korea Research Institute of Chemical Technology.

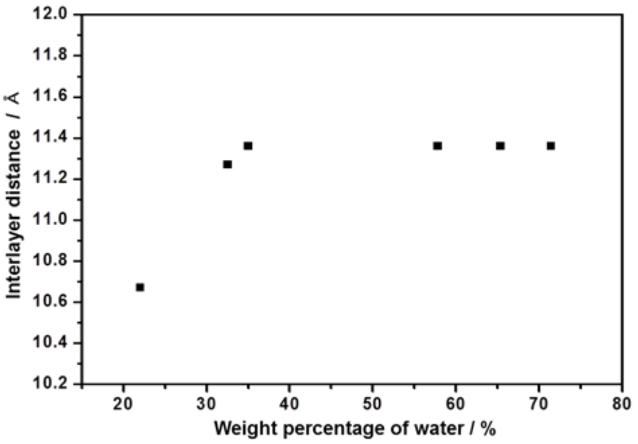

Fig. 2 Interlayer distance of GO in relation to the weight percentage of water. The interlayer was saturated to 35 wt% water.

To achieve water swelling of the GO, dried GO was placed in the vacuum oven with distilled water and then the air was evacuated by vacuum pump. In the oven, the relative humidity reached 100 % and vaporized water diffused into the GO, causing it to swell. The exact amount of water added to the GO plays an important role in determining whether the hydrates formed, come from confined or bulk spaces. The interlayer distance within the GO changes depending on the amount of added water and resulting interlayer spacing reaches maximum at a water concentration of 35 wt% (Fig. 2). Accordingly, all the experiments were carried out at this saturated water concentration, complying with the following procedure for gas hydrate formation. The swollen GO (1.5 g) was loaded into a high-pressure reactor with 11 mL internal volume, pressurized by gas injected at room temperature, and then placed in a cooling bath at 243 K for 24 h. All the gases were supplied by Special Gas, Korea with 99.995% purity and were used in all the experiments without any further treatment. The high pressure cell was equipped with a four-wire type Pt-100Ω probe for the temperature sensing and pressure transducer (Druck, PMP5073) with accuracy ± 0.2 % in the ranges of 0–25 Mpa. The temperature was maintained with a circulating bath (Jeio Tech., RW-2040G) with a stability of ± 0.05 K. And the pressure and temperature measured from the apparatus were calibrated using the thermometer and pressure gauge calibrated by Korea Research Institute of Standards and Science, by which the uncertainties of equilibrium temperature (± 0.1 K) and pressure (± 0.01 MPa) were achieved. The pressure of the injected gas was controlled by a syringe pump connected to both gas cylinder and high pressure cell. For the P-T trace curve we followed isochoric cooling and heating procedures with a rate of -1 K/h and 0.1 K/h, respectively. All the temperatures and pressures during measurement were recorded by a data acquisition system at every 20 sec. The reactor was equipped with a mechanical stirrer, as well as with P and T detectors for

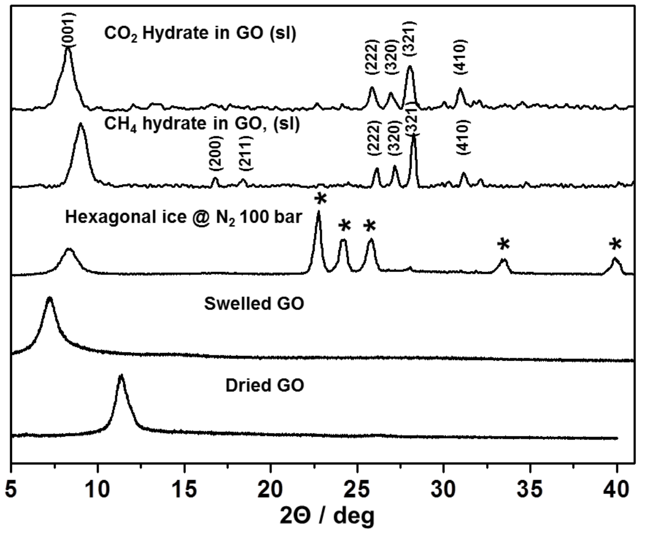

Fig.3 XRD of water-swollen GO after pressurization with various gases. Asterisks indicate diffraction from hexagonal ice.

continuous stirring and data acquisition. For the XRD measurements, all the samples exposed to gas were rapidly quenched using liquid nitrogen. These samples were finely ground to particles smaller than 200 um and placed in a sample loader. Powder x-ray diffraction was conducted using a Low-Temperature XRD (D/MAX, Rigaku) with CuK radiation (λ = 1.5406 Å) at a generator voltage of 40 kV and generator current of 300 mA. XRD measurement was performed using 0.05 steps at 93 K. The X-ray photoelectron spectroscopy analysis was performed using a Sigma Probe (Thermo VG Scientific). In this experiment, GO was dispersed in water, dropped onto Si substrate, and then dried to form a thin film.

Results and discussions

For polyhedral cage formation, the main concern is to secure the least dimension for guest occupancy in stringently confined space. Accordingly, it is meaningful to check whether GO interlayers can provide a space sufficient for the anticipated guest molecules. We note that the layer thickness and interlayer spacing of GO are 6 and 10.5 Å, respectively. Thus the inner effective space for intercalating molecules becomes 4.5 Å, but this is too narrow to encompass a small 5^{12} cage (~8 Å). Instead, it is the GO interlayer that can absorb and intercalate water, in which CO_2 can be dissolved.[8] At this point, it needs to be emphasized that the gas hydrate can only form in the non-interlamellar voids of GO, as shown in Fig. 1c.

The XRD was first used to observe any possible structural change of water-swelled GO (Fig. 3). The structure analysis confirmed the formation of gas hydrates when pressurized with gas molecules of CO_2, CH_4, and N_2. The GO showed a main peak at 2Θ near 10 degrees, which corresponds to diffraction from the layered GO structure and d-spacing identical with the interlayer distance between GO sheets. The genuine interlayer distance of 7 Å without water, consistently increased with the amount of water absorbed but ceased swelling, after reaching 11.35 Å, at a water content of 35 wt% (Fig. 2). At the present stage, the key questions that need to be addressed are whether physical variables such as pressure and temperature, as well as chemical interactions and molecular details of guest-host components, really affect water structures in specified spaces. Fig. 3 shows that the swollen GO pressurized with CO_2 and CH_4 at pressure above 2 MPa, evolved four strong peaks of (222), (320), (321) and (410) corresponding to sI. In contrast, at pressure lower than 2 MPa, the hexagonal-ice phase was observed to predominate.[8] Here, it is interesting to see that the swollen GO pressurized with N_2 at 10 MPa failed to make any suitable hydrate structures; instead, hexagonal ice formed. The reactor containing swollen GO was pressurized by CO_2, CH_4 and N_2 gases, which made the inner pressure reach 2.2 , 4.7 and 15 MPa, respectively, with successive cooling and heating. A rapid pressure drop was observed for CO_2 and CH_4 during cooling, which naturally confirms the formation of gas hydrate. In contrast, a detectable pressure drop was not observed for N_2 gas during cooling, even at pressures much higher than the corresponding equilibrium pressure of pure bulk N_2 hydrate.[9] The XRD results in Fig. 3 also confirm the nonexistence of N_2 hydrate in swollen GO. Interestingly, two notable features were observed along the heating line of the GO matrix, which have never before been shown in bulk hydrates. First, the pressure along the cooling line should generally match that along the heating line at a specified equilibrium temperature, but for GO-CO_2, the two lines mismatched (Fig. 4a). It is interesting to see

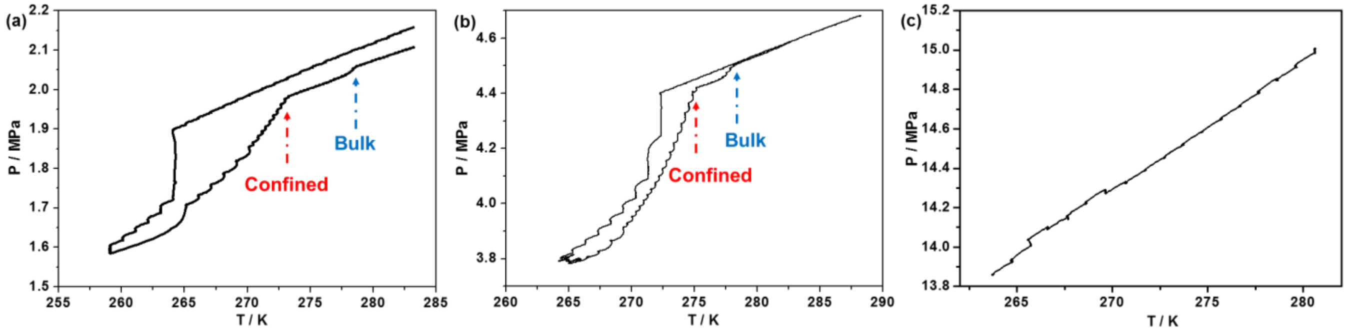

Fig. 4 Pressure and temperature trace curves of (a) CO_2, (b) CH_4, and (c) N_2, in which red and blue arrows indicate confined and bulk hydrate phase, respectively.

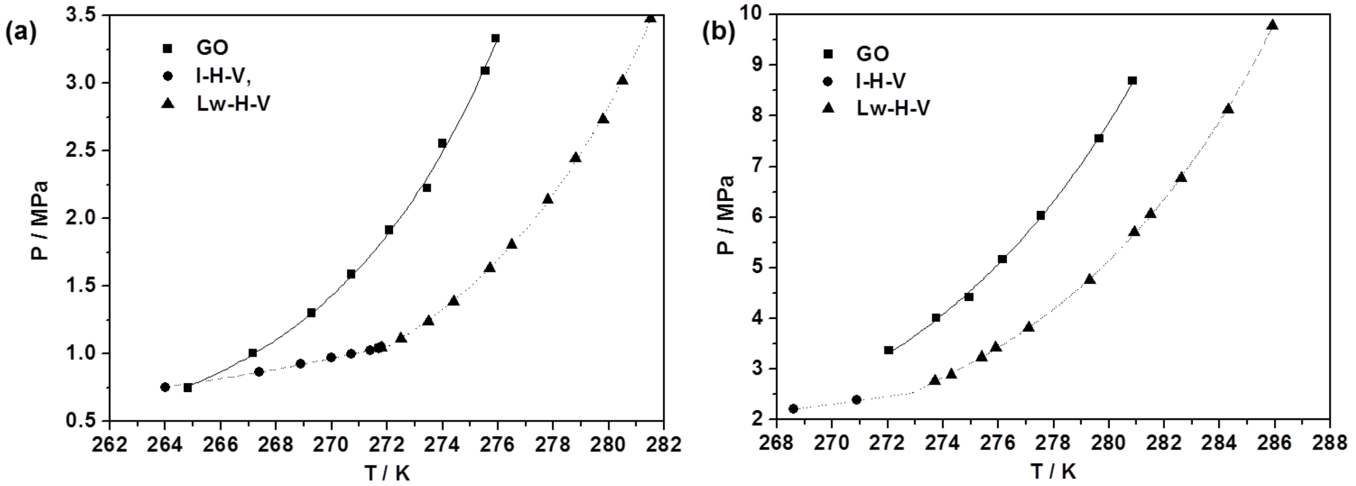

Fig. 5 Hydrate phase equilibria for (a) CO2 and (b) CH4 hydrate in GO. The black squares and triangles indicate that of bulk hydrate, where the data reported by Larson (CO_2),[10] and Deaton and Frost (CH_4) were represented.[11]

that this pressure gap was not observed in the test using CH_4 as can be seen in Fig. 4b. Such abnormal PT behavior of a hydrophilic CO_2 gas could be attributed to much larger amounts of CO_2 intercalated in the swollen interlayers of GO than of CH_4, N_2 and H_2 gases.[8] Second, both GO-CO_2 and GO-CH_4 comprise two different hydrate phases along the dissociating heating line. The one at higher pressure and temperature corresponds to bulk hydrate, while the other one shows more inhibited hydrate. The bulk hydrate phase is attributed to excess water, but its amount is negligible when compared with that of the inhibited hydrate phase as can be clearly observed by a large pressure increase between bulk and inhibited hydrate phase along the dissociation line. The phase equilibrium data of the inhibited CO_2 and CH_4 hydrate phases in GO are given in Table 1 and plotted in Fig. 5a and 5b, respectively, confirming their inhibition tendency. Here, we note that the quadruple point at which ice, hydrate, liquid water and gas phases coexist did not appear in GO-gas systems in the experimental temperature range because pore confinement induces water confined in GO to crystallize at temperatures below 253 K.

At this point it is of considerable interest to determine where the strong inhibition originated. First, we assumed two possibilities: a confinement effect in GO and an effect inherent in the properties of GO. However, it was not clear which one is most responsible for inducing inhibition. To clarify the situation, first 20 wt% GO was dissolved (dispersed) in water for 2 h with strong sonication, thereby separating stacked GO sheets into pieces of single GO sheets and eventually causing the confining effect to be lost. Subsequently, we placed the 20-wt% GO in a reactor equipped with a stirring machine and then pressurized it with CH_4 at 8 MPa and 285 K. From the P-T trace curve shown in Fig. 6, we determine the phase equilibrium point at 282.9 K and 7.76 MPa, which indicates a slight inhibition in comparison with pure CH_4 hydrate in bulk state (283.9 K), but a strong inhibition appeared in water-swollen GO (279.9 K). Considering the fact that a stronger inhibition occurred at the severely confined space, we might suggest with reasonable validity that the spatially confinement more strongly influences than surface property on hydrate structuring. The pores are known to cause water activity to be lower and hydrate inhibition to be stronger.[12] In water-

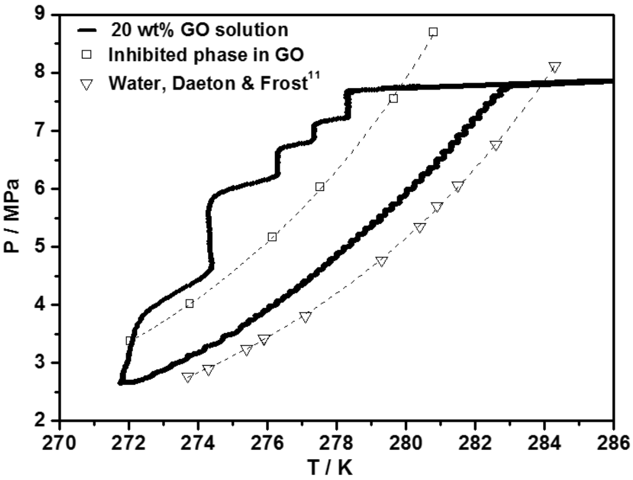

Fig. 6 Pressure and temperature trace curve of CH_4 in 20 wt% GO solution. Open squares and triangles represent phase equilibrium points of inhibited phase in the GO and bulk systems, respectively.

TABLE 1. Hydrate phase equilibria for CO_2 and CH_4 hydrate in GO

CO_2		CH_4	
T / K (±0.1)	P / MPa(±0.01)	T / K (±0.1)	P / MPa(±0.01)
264.9	0.8	272.05	3.37
267.2	1.0	273.75	4.01
269.3	1.3	274.95	4.42
270.8	1.6	276.15	5.17
272.1	1.9	277.55	6.03
273.5	2.2	279.65	7.55
273.9	2.6	280.85	8.69
275.6	3.1		
276.0	3.3		

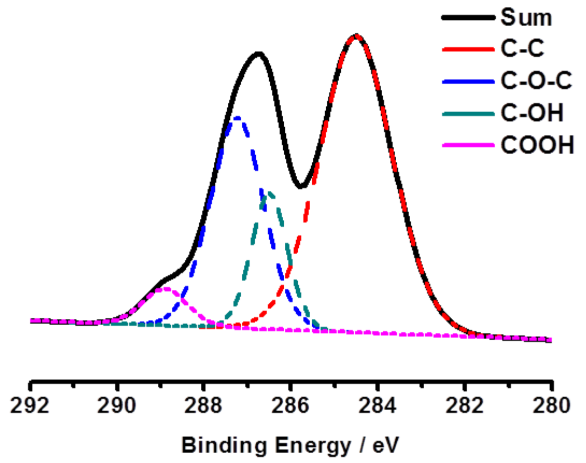

Fig. 7 X-ray photoelectron spectroscopy analysis of GO. Peaks corresponding to OH, COOH and COC functional groups are indicated.

swollen GO, the water activity is greatly lowered by pores and by the strong interaction of water with GO surfaces. As shown by the XPS analysis in Fig. 7, the GO used in the experiments contained ether and hydroxyl groups attached to the basal plane of the GO sheet, and carboxylic ones to the edge of the GO sheet. These functional groups make GO surfaces highly hydrophilic and cause further strong water adsorption.

On hydrophilic surfaces, water molecules are localized due to the interaction between surfaces and neighboring water molecules by hydrogen bonding and steric factors.[13] We need to note again that the functional groups can be partially dissolved in water, and then make an acidic environment that inhibits the hydrate phase.

Conclusion

In this paper, we attempted to examine the roles of pores and surfaces in the formation of gas hydrate and its thermodynamic behavior. Contrary to CO_2 and CH_4 that formed hydrate structure in non-interlamellar voids of GO, N_2 didn't shows hydrate structure in our experimental condition (up to 15 MPa). Nano-sized small space and highly-functionalized surface of GO make the phase behaviour of gas hydrate formed in GO to be strongly inhibited. This result suggests new possibility that tuning the surface of porous materials for diverse applications in the fields of inclusion chemistry, including gas storage and separation, e.g. immobilizing THF molecules on the surface of porous materials to overcome the thermodynamic disadvantage of hydrate formation in nanoporous materials.

Acknowledgements

The acknowledgements come at the end of an article after the conclusions and before the notes and references. This research was funded by the following grants: 1) National Research Foundation of Korea (NRF) grant funded by the Ministry of Science, ICT and Future Planning, Korea (MSIP, NRF-2012R1A2A1A01003537); 2) A grant funded by the Center for Advanced Soft Electronics under the Global Frontier Research Program of the Ministry of Science, ICT and Future Planning, Korea (MSIP, NRF-2012M3A6A5055744); 3) The National Research Foundation Korea (NRF) funded by the Korean government (MEST) (No. 2013-059738). We also gratefully acknowledge the Pohang Accelerator Laboratory (Beamline 9B-HRPD). H.K.L., J.J., and H.K. acknowledge support by the Nano·Material Technology Development Program (2012M3A7B4049807), and also the Global Frontier R&D Program (2013-073298) at the Center for Hybrid Interface Materials (HIM), through the National Research Foundation of Korea (NRF) funded by the Ministry of Science, ICT and Future Planning.

Notes and references

[a] Graduate School of EEWS, Korea Advanced Institute of Science and Technology, 291 Daehak-ro, Yuseong-gu, Daejeon 305-701, South Korea
[b] Department of Chemical and Biomolecular Engineering, Korea Advanced Institute of Science and Technology, 373-1 Guseong-dong, Yuseong-gu, Daejeon 305-701, South Korea
★E-mail: H. Lee, H_lee@kaist.ac.kr; H. T. Jung, heetae@kaist.ac.kr

‡These authors contributed equally.

References

1 (a) H. Kanda, Economic study on natural gas transportation with natural gas hydrate (NGH) pellets., 23rd World Gas Conference, Amsterdam 2006; (b) J. S. Gudmundsson, O. F. Graff, Hydrate non-pipeline technology for transport of natural gas , 22nd World Gas Conference, Tokyo, 2003.

2 (a) A. Eslamimanesh, A. H. Mohammadi, D. Richon, P. Naidoo, D. Ramjugernath, *J. Chem. Thermodyn.*, 2012**,** **46**, 62–71; (b) V. M. Vorotyntsev, V. M. Malyshev, *J. Phys. Chem. A*, 2011, **85**, 1990–1994; (c) Y. Seo, H. Tajima, A. Yamasaki, S. Takeya, T. Ebinuma, F. Kiyono, *Environ. Sci. Technol.*, 2004**,** **38**, 4635–4639; (d) D. L. Zhong, N. Daraboina, P., Englezos, *Fuel*, 2013, **106**, 425–430; (e) V. M. Vorotyntsev, V. M. Malyshev, P. G. Taraburov, G. M. Mochalov, *Theor. Found. Chem. Eng.*, 2001, **35**, 513–515. (f) I. Cha, S. Lee, J. D. Lee, G. W. Lee, Y. Seo, *Environ. Sci. Technol.*, 2010, **44**, 6117–6122.

3 (a) C. G. Xu, S. H. Zhang, J. Cai, Z. Y. Chen, X. S. Li, *Energy*, 2013, **59**, 719–725; (b) Y. T. Seo, S. P. Kang, H. Lee, C. S. Lee, W. M. Sung, *Korean J. Chem. Eng.*, 2000, **17**, 659–667; (c) S. P. Kang, H. Lee, *Environ. Sci. Technol.*, 2000, **34**, 4397–4400. (d) J. Gholinezhad, A. Chapoy, B. Tohidi, *Chem. Eng. Res. Des.*, 2011, **89**, 1747–1751.

4 (a) Y. T. Seo, I. L. Moudrakovski, J. A. Ripmeester, J. W. Lee, H. Lee, *Environ. Sci. Technol.*, 2005, **39**, 2315–2319; (b) Y. Seo, S. P. Kang, *Chem. Eng. J,* 2010, **161**, 308–312; (c) J. Park, Y. T. Seo, J. W. Lee, H. Lee, *Catal. Today*, 2006, **115**, 279–282; (d) Y. C. Song, X. J. Wan, M. J. Yang, L. L. Jiang, Y. Liu, B. L. Dou, J. F. Zhao, S. R. Wang, *Energy Fuels*, 2013, **27**, 3341–3348.

5 L. Mu, B. Liu, H. Liu, Y. T. Yang, C. Y. Sun, G. J. Chen, *J. Mater. Chem.* 2012, **22**, 12246-12252.

6 D. R. Dreyer, S. Park, C. W. Bielawski, R. S. Ruoff, *Chem. Soc. Rev.*, 2010, **39**, 228–240.

7 (a) A. Lerf, A. Buchsteiner, J. Pieper, S. Schottl, I. Dekany, T. Szabo, H. P. Boehm, *J. Phys. Chem. Solids*, 2006, **67**, 1106–1110; (b) S. Cerveny, F. Barroso-Bujans, A. Alegria, J. Colmenero, *J. Phys. Chem. C*, 2010, **114**, 2604–2612; (c) J. Yu, M. Gu, C. Bian, X. B. Xu, T. B.

Tang, *Carbon*, 2013, **61**, 367–372; (d) A. Buchsteiner, A. Lerf, J. Pieper, *J. Phys. Chem. B*, 2006, **110**, 22328–22338.

8 Kim, D. Kim, D.W., Lim, H.K. Jeon, J. Kim, H. Jung, H.T. Lee, H. *J. Phys. Chem. C* 2014, DOI: 10.1021/jp5026762.

9 J. B. Klauda, S. I. Sandler, *Chem. Eng. Sci.*, 2003, **58**, 27–41.

10 Larson, S.D. in *Phase Studies of the Two Component Carbon Dioxide-water System Involving the Carbon Dioxide Hydrate*, University of Illinois, Urbana, IL, U.S.A. 1955

11 W. M. Deaton, E. M. Frost, in *Gas hydrates and their relation to the operation of natural-gas pipe lines*, Bureau of Mines Monograph 8, U.S.A. 1946

12 (a) S. Lee, Y. Seo, *Energy Fuels*, 2010, **24**, 6074–6080; (b) Y. Seo, H. Lee, *J. Phys. Chem. B*, 2003, **107**, 889–894; (c) M. A. Clarke, M. Pooladi-Darvish, P. R. Bishnoi, *Ind. Eng. Chem. Res.*, 1999, **38**, 2485–2490.

13 C. Y. Ruan, V. A. Lobastov, F. Vigliotti, S. Y. Chen, A. H. Zewail, *Science*, 2004, **304**, 80–84.